Spin-valley Hall conductivity of doped ferromagnetic silicene under strain

Bahram Shirzadi[1] and Mohsen Yarmohammadi[2,†]

[1] Department of Physics, Razi University, Kermanshah, Iran

[2] Young Researchers and Elite Club, Kermanshah Branch, Islamic Azad University, Kermanshah, Iran

(Received 8 September 2016; revised manuscript received 28 September 2016; published online 30 November 2016)

The spin-valley Hall conductivity (SHC-VHC) of two-dimensional material ferromagnetic graphene's silicon analog, silicene, is investigated in the presence of strain within the Kubo formalism in the context of the Kane–Mele Hamiltonian. The Dirac cone approximation has been used to investigate the dynamics of carriers under the strain along the armchair (AC) direction. In particular, we study the effect of external static electric field on these conductivities under the strain. In the presence of the strain, the carriers have a larger effective mass and the transport decreases. Our findings show that SHC changes with respect to the direction of the applied electric field symmetrically while VHC increases independently. Furthermore, the reflection symmetry of the structure has been broken with the electric field and a phase transition occurs to topological insulator for strained ferromagnetic silicene. A critical strain is found in the presence of the electric field around 45%. SHC (VHC) decreases (increases) for strains smaller than this value symmetrically while it increases (decreases) for strains larger than one.

Keywords: ferromagnetic silicene, Kubo formalism, strain, spin-valley conductivity

PACS: 72.25.Dc, 77.80.bn, 77.80.bn, 77.80.B– **DOI:** 10.1088/1674-1056/26/1/017203

1. Introduction

Significant interest has been attracted to study physical properties of new two-dimensional (2D) materials with the honeycomb lattice both experimentally and theoretically after the discovery of the first real 2D-material graphene in 2004,[1] for example, hexagonal boron-nitride (h-BN), MoS_2, and recently a monolayer of silicon, known as silicene. Although these materials have a honeycomb lattice, their properties are different.[2–7] Graphene is gapless and this creates a problem for using graphene as a highly motivated new electronic device.[8–10] The band gap is a measurement of the threshold voltage and on-off ratio of the field effect transistors.[11,12] It is desirable to have a band gap in materials in addition to their novel features. Unlike graphene, according to Fig. 1, silicene has a hexagonal atomic arrangement but has a buckled configuration because of its large ionic radius[13–16] such that its sublattices (A and B) sit in two parallel planes with a vertical distance 0.46 nm.[17,18] The low-energy dynamics of fermions in graphene is described by the Dirac Hamiltonian in the vicinity of K and K' valleys, but in silicene, due to the strong spin–orbit (SO) interaction, the carriers are massive with an energy gap around 1.55 meV.[19,20] This gap can be modulated via an applied perpendicular electric field to the layer, which leads to many attractive properties of silicene.[21–28] On the other hand, strain can change many features of 2D-materials.[29] In graphene, the Dirac points remain at K and K' under a biaxial strain, but they are affected by the strain along different directions.[30–33] Contrary to graphene, both σ^* and π^* bands of silicene are more sensitive to strain.[34–38] For example, silicene becomes metallic under a biaxial strain smaller than 12%[34–36] and it turns into a metal under a strain larger than 12% (14%) along the AC (ZZ) directions.[38] As an important point, the strong SO interaction in silicene couples spin and valley degrees of freedom. Nowadays, spin and valley physics has attracted the attention of researchers because of the spintronic and valleytronic applications. Also the degeneration of valleys in the limit of zero doping due to the time reversal symmetry causes the further investigation of spin and valley transports of Dirac fermions in 2D graphene-like materials.[39–45] On the other hand, strain engineering is one of the important topics as an effective case on the spin and valley properties of 2D-materials.[46–50] In silicene, a phase transition from a quantum spin Hall state (for absolute value of energy gap smaller than the SO strength) to a band insulating state (for absolute value of energy gap larger than the SO strength) by tuning the SO interaction strength and energy gap has been observed.[51–56] It leads to the quantum spin Hall effect (SHE) and quantum valley Hall effect (VHE), which are examined by an ac electric field.[53,56] However, the SHC-VHC of silicene under strain still remains to be studied.

In this work, we investigate the SHC-VHC of a ferromagnetic silicene under strain at Dirac points. Our system is ferromagnetic with an exchange field M. Also at given strain modulus and direction of the applied strain, SHC/VHC are studied with an electric field. The Kubo technique is carried out with the Kane–Mele Hamiltonian. The outline of this paper is as

†Corresponding author. E-mail: m.yarmohammadi69@gmail.com

© 2017 Chinese Physical Society and IOP Publishing Ltd

follows. Section 2 describes the Hamiltonian and calculation details. In Section 3, we show the SHC/VHC of the system under strain. In Section 4, the numerical results are investigated. Finally, Section 5 gives the summary of the paper.

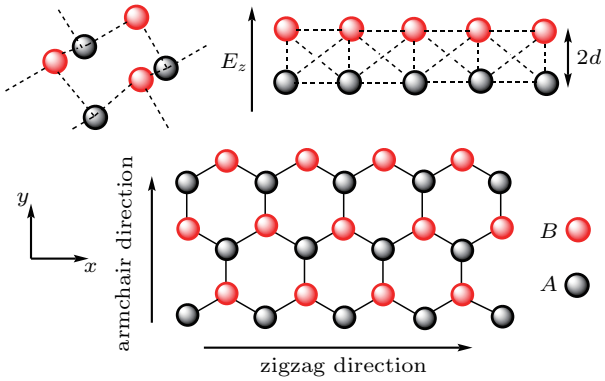


Fig. 1. (color online) Schematic illustration of silicene sheet. The A and B sites are separated by a distance $2d$ in the electric field E_z.

2. The effective Hamiltonian model

In this section, we present the effective Hamiltonian model to describe the low-energy dynamics of carriers in a ferromagnetic silicene which is subjected to a perpendicular uniform electric field[19,57]

$$H_{\tau,s_z} = \hbar v_{\rm F}(k_x\sigma_x - \tau k_y\sigma_y) - \tau s_z\Delta_{\rm SO}\sigma_z + \Delta_z\sigma_z - Ms_z. \quad (1)$$

In our model, the wave functions in the sublattice pseudospin space in terms of the A and B sublattice components can be defined as $\Psi_{\tau,s_z} = \{\psi^A_{\tau,s_z}, \psi^B_{\tau,s_z}\}^{\rm T}$. The first term is the normal graphene Hamiltonian (Dirac Hamiltonian) at the Dirac cone approximation for both valleys K and K', which is indexed by $\tau = +\,(-)$, and $v_{\rm F}$ is the Fermi velocity of silicene's carriers. The in-plane momentum $\boldsymbol{k} = (k_x, k_y)$ measured from the hexagonal first Brillouin zone and σ_i $(i = x, y, z)$ are the Pauli matrices. The second term is the Kane–Mele Hamiltonian for the intrinsic SO coupling. For silicene, $\Delta_{\rm SO} = 3.9$ meV[19] is the SO coupling strength and $s_z = +\,(-)$ is defined for spin up (down). The third term describes the on-site potential difference between A and B sublattices with $\Delta_z = E_z d$, where E_z is the applied perpendicular electric field and $2d = 0.46$ nm is the vertical distance of the sublattice's planes, as shown in Fig. 1. If silicene is deposited on the surface of a magnetic insulator substrate, an exchange magnetization can be induced in silicene with $M = \Delta_{\rm SO}/2$ as the exchange field.[58,59] The effect of strain on the Hamiltonian is given by the two-dimensional reductions of the strain tensor[33,60]

$$\varepsilon = \epsilon \begin{pmatrix} \cos^2\theta - \nu\sin^2\theta & (1+\nu)\cos\theta\sin\theta \\ (1+\nu)\cos\theta\sin\theta & \sin^2\theta - \nu\cos^2\theta \end{pmatrix}, \quad (2)$$

where θ denotes the angle of the applied strain with respect to the x axis direction, ε is the strain modulus, and $\nu = 0.62$ is Poisson's ratio from *ab initio* calculations for silicene.[61] In our calculations, $\theta = 0$ refers to the strain along the AC direction. Thus, we have considered our calculations based on the converted nearest neighbors vectors after strain.

The Hamiltonian under strain in Eq. (1) can be written as $H_{\tau,s_z}(\boldsymbol{k}) = U^\dagger(\theta)H^0_{\tau,s_z}(\boldsymbol{k})U(\theta)$, in which

$$U(\theta) = \begin{pmatrix} 1 & 0 \\ 0 & {\rm e}^{-{\rm i}\theta} \end{pmatrix}$$

is the unitary matrix performing a rotation in the sublattice space[62] and

$$H^0_{\tau,s_z}(\boldsymbol{k}) = \begin{pmatrix} \Delta_z - \tau s_z\Delta_{\rm SO} - Ms_z & k_x(1-\lambda_x\varepsilon) + {\rm i}\tau k_y(1-\lambda_y\varepsilon) \\ k_x(1-\lambda_x\varepsilon) - {\rm i}\tau k_y(1-\lambda_y\varepsilon) & -\Delta_z + \tau s_z\Delta_{\rm SO} - Ms_z \end{pmatrix},$$

where $\lambda_x = 2.2$ and $\lambda_y = -1.3$ are the logarithmic derivatives of the nearest-neighbor hopping with respect to the lattice parameter ($a = 0.386$ nm) at $\varepsilon = 0$ along the x and y directions, respectively.[63] Finally, the effective Hamiltonian is given by

$$H_{\tau,s_z}(\boldsymbol{k}) = \begin{pmatrix} \Delta_z - \tau s_z\Delta_{\rm SO} - Ms_z & \hbar v_{\rm F}{\rm e}^{-{\rm i}\theta}\Big(k_x(1-\lambda_x\varepsilon) + {\rm i}\tau k_y(1-\lambda_y\varepsilon)\Big) \\ \hbar v_{\rm F}{\rm e}^{{\rm i}\theta}\Big(k_x(1-\lambda_x\varepsilon) - {\rm i}\tau k_y(1-\lambda_y\varepsilon)\Big) & -\Delta_z + \tau s_z\Delta_{\rm SO} - Ms_z \end{pmatrix}. \quad (3)$$

The eigenvalues of the above Hamiltonian are described by the following electronic bands:

$$E^{\pm}_{\tau,s_z}(k) = \pm\sqrt{\Delta^2_{\tau,s_z} + (\hbar v_{\rm F}k)^2} - Ms_z, \quad (4)$$

where $+\,(-)$ refers to the conduction (valance) bands, $\Delta_{\tau,s_z} = \Delta_z - \tau s_z\Delta_{\rm SO}$, and $k = \sqrt{k'^2_x + k'^2_y}$, with $k'_x = k_x(1-\lambda_x\varepsilon)$ and $k'_y = k_y(1-\lambda_y\varepsilon)$. The corresponding wave functions are given by

$$\Psi^{\pm}_{\tau,s_z} = \frac{{\rm e}^{{\rm i}\boldsymbol{k}\cdot\boldsymbol{r}}}{\sqrt{2\chi_{\tau,s_z}}} \begin{pmatrix} \sqrt{\chi_{\tau,s_z} \mp \Delta_{\tau,s_z}} \\ \pm\sqrt{\chi_{\tau,s_z} \pm \Delta_{\tau,s_z}}\,{\rm e}^{-{\rm i}\tau\varphi_k} \end{pmatrix}, \quad (5)$$

where $\chi_{\tau,s_z} = \sqrt{\Delta^2_{\tau,s_z} + (\hbar v_{\rm F}k)^2}$ and $\varphi_k = \arctan(k'_y/k'_x)$. By these expressions, SHC and VHC of this system are calculated in the next section.

3. Spin/valley Hall conductivity

The DC transverse Hall conductivity of doped ferromagnetic silicene under strain σ_{xy} within the Kubo formalism can be written as[64,65]

$$\sigma_{xy}^{\tau,s_z} = -\mathrm{i}\frac{e^2\hbar}{A}\sum_{\boldsymbol{k}}\frac{f(E_{\tau,s_z}^{+})-f(E_{\tau,s_z}^{-})}{(E_{\tau,s_z}^{+}-E_{\tau,s_z}^{-})^2} \times \langle\Psi_{\tau,s_z}^{+}|v_x|\Psi_{\tau,s_z}^{-}\rangle\langle\Psi_{\tau,s_z}^{-}|v_y|\Psi_{\tau,s_z}^{+}\rangle, \quad (6)$$

where $A=1$ is the area of the system in our calculations and $v_{x(y)}$ are the velocity components that can be calculated from $v_i=(1/\hbar)(\partial H/\partial k_i)$. Also

$$f(E_{\tau,s_z}^{\pm}) = 1/(1+\mathrm{e}^{(E_{\tau,s_z}^{\pm}-\mu)/k_{\mathrm{B}}T})$$

is the Fermi–Dirac distribution function, where k_{B} is the Boltzmann constant and μ is the chemical potential. The chemical potential at zero temperature is equal to the Fermi energy. Our investigations are carried out at zero temperature. The final relation for the DC transverse Hall conductivity of this system is obtained as

$$\sigma_{xy}^{\tau,s_z} = -\tau e^2 v_{\mathrm{F}}^2\hbar\Delta_{\tau,s_z}\sum_{\boldsymbol{k}}\frac{\sinh\{(\sqrt{\Delta_{\tau,s_z}^2+(\hbar v_{\mathrm{F}}k)^2})/k_{\mathrm{B}}T\}}{(\chi_{\tau,s_z}^3)\left(\cosh\{(\sqrt{\Delta_{\tau,s_z}^2+(\hbar v_{\mathrm{F}}k)^2})/k_{\mathrm{B}}T\}+\cosh(Ms_z+\mu)\right)}. \quad (7)$$

After solving this relation for arbitrary parameters including M, Δ_z, μ, and ε, the SHC/VHC of this system can be obtained as follows:[64–67]

$$\sigma_{xy}^{s} = \frac{\hbar}{2e}\sum_{\tau,s_z}s_z\sigma_{xy}^{\tau,s_z} = \frac{\hbar}{2e}(\sigma_{xy}^{+,+}+\sigma_{xy}^{-,+}-\sigma_{xy}^{+,-}-\sigma_{xy}^{-,-}), \quad (8)$$

$$\sigma_{xy}^{v} = \frac{1}{2e}\sum_{\tau,s_z}\tau\sigma_{xy}^{\tau,s_z} = \frac{1}{2e}(\sigma_{xy}^{+,+}+\sigma_{xy}^{+,-}-\sigma_{xy}^{-,+}-\sigma_{xy}^{-,-}). \quad (9)$$

In the next section, by setting $k_{\mathrm{B}}=v_{\mathrm{F}}=1$, the results of SHC and VHC are presented in detail.

4. Numerical results

The band structures of doped ferromagnetic silicene with $\mu=\Delta_{\mathrm{SO}}$ over the first Brillouin zone for K (K') valleys under strain ε with a given applied electric field, $\Delta_z/\Delta_{\mathrm{SO}}=0.75$, are shown in Fig. 2. Also different kinds of spin configurations have been considered. Because of the unique band structure of silicene, a symmetry between the results of valleys and spins is seen. Plots are reflected with respect to the $(E(k)\pm\mu)/\Delta_{\mathrm{SO}}=0$ by exchanging the spin up and down. The $\varepsilon=0$ (black solid lines), $\varepsilon=5\%$ (red dashed lines), $\varepsilon=10\%$ (green dotted lines), and $\varepsilon=15\%$ (violet dotdashed lines) are the various values of the strain modulus. In the presence of an applied external electric field, the slope of bands is decreased with strain for all kinds of configurations, which leads to the increase of electron and hole effective masses $(1/m^*=\hbar^{-1}\partial^2E(K)/\partial^2k)$ and the decrease of transport. Also a non-vanishing density of states at the Fermi energy is found. Surprisingly, the direct band gap due to the breaking of the inversion symmetry remains at the Fermi level with respect to the chemical potential, the system is a semimetal for all strains in the presence of the electric field, and there is no transition which is in qualitative agreement with the results of recent works.[21,66,67] This can be understood from the fact that the detected potentials by silicon atoms at the A and B sublattices are different. In other works, a semimetal–metal transition occurs in the absence of an electric field.[68,69] Spin splitting for $\Delta_z/\Delta_{\mathrm{SO}}=0.75$ ($\Delta_z<\Delta_{\mathrm{SO}}$) occurrs in Figs. 2(a) and 2(b) for valley K and Figs. 2(c) and 2(d) for valley K', which is consistent with the results by Nicol and Tabert.[70] These behaviors can affect the SHC and VHC of the system.

In Fig. 3, the DC transverse Hall conductivity as a function of the electric field for various strain moduli is plotted at a fixed doping $\mu/\Delta_{\mathrm{SO}}=1$. In Figs. 3(a) and 3(b), for valley K with spin up (down), by increasing the strain for $\Delta_z<\Delta_{\mathrm{SO}}(-\Delta_{\mathrm{SO}})$, the conductivity decreases due to the increase of the effective mass of the carriers, and at $\Delta_z=\Delta_{\mathrm{SO}}(-\Delta_{\mathrm{SO}})$, it becomes zero and then increases; this can be analyzed from the symmetry between spin up and down. Another point is related to the increase of the conductivity with the electric field. The electric field acts as an external perturbation and leads to the increase of the scattering rate of carriers and the conductivity. For valley K' with spin up (down), because of the symmetry between valleys, an inverse result is expected. By increasing the strain modulus, the conductivity increases for $\Delta_z<-\Delta_{\mathrm{SO}}(\Delta_{\mathrm{SO}})$ and goes to zero at $\Delta_z=-\Delta_{\mathrm{SO}}(\Delta_{\mathrm{SO}})$, then decreases as shown in Figs. 3(c) and 3(d). On the other hand, the conductivity decreases in valley K' with the electric field. These behaviors lead to a general treatment for SHC and VHC. In Fig. 4, SHC is plotted as a function of the electric field and decreases (increases) for $\Delta_z<0$ ($\Delta_z>0$) due to the symmetric direction of the applied electric field with respect to the spins. Also when the strain modulus increases, because of the inversion symmetry breaking between sublattices, at a given electric field, SHC decreases and has a stronger oscillation than the noninteracting case. These results are in agreement with the obtained results by Tahir *et al.*[71] The VHC increases with the electric field, as shown in Fig. 5, but decreases (increases) with the strain at $\Delta_z<0$ ($\Delta_z>0$).

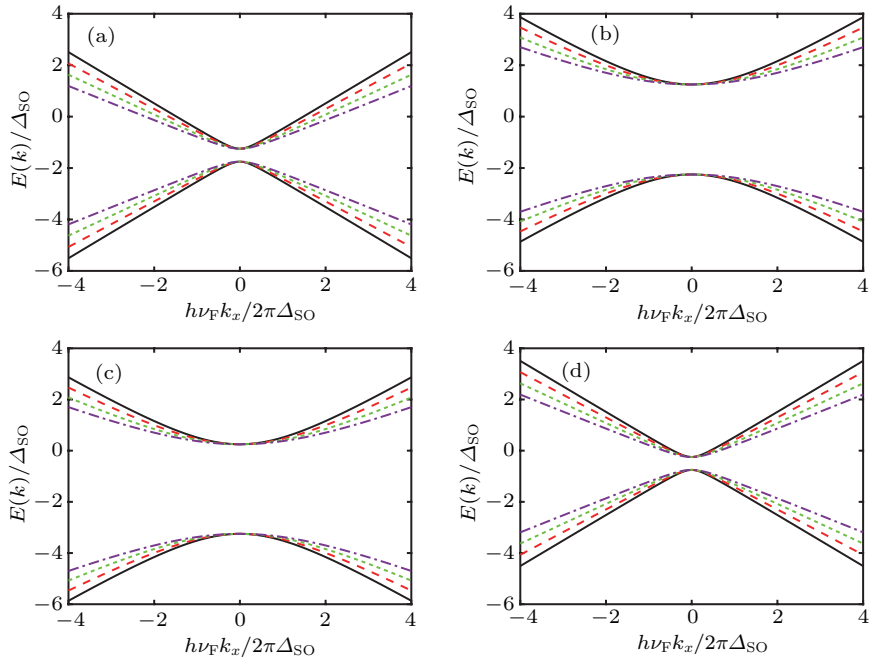


Fig. 2. (color online) The energy spectrum of ferromagnetic silicene with $M = \Delta_{SO}/2$ and $\Delta_z/\Delta_{SO} = 0.75$ for different strain modulus: $\varepsilon = 0$ (black solid lines), $\varepsilon = 5\%$ (red dashed lines), $\varepsilon = 10\%$ (green dotted lines), and $\varepsilon = 15\%$ (violet dotdashed lines) at a fixed chemical potential $\mu/\Delta_{SO} = 1$. (a) Valley K, $s_z = +$; (b) valley K, $s_z = -$; (c) valley K', $s_z = +$; (d) valley K', $s_z = -$.

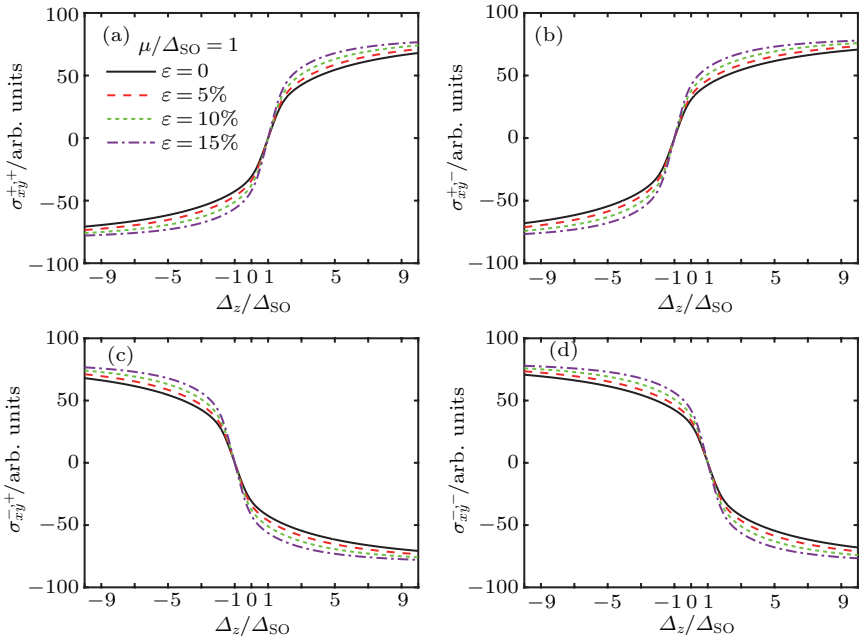


Fig. 3. (color online) The DC transverse Hall conductivity ((a) $\sigma_{xy}^{+,+}$, (b) $\sigma_{xy}^{+,-}$, (c) $\sigma_{xy}^{-,+}$, (d) $\sigma_{xy}^{-,-}$) as a function of the applied electric field for different strain modulus and all spin and valley configurations with $\mu/\Delta_{SO} = 1$.

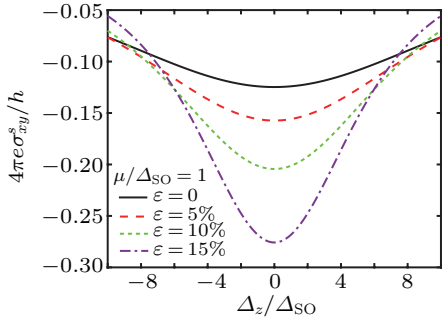


Fig. 4. (color online) SHC as a function of the electric field for different strain modulus at $\mu/\Delta_{SO} = 1$.

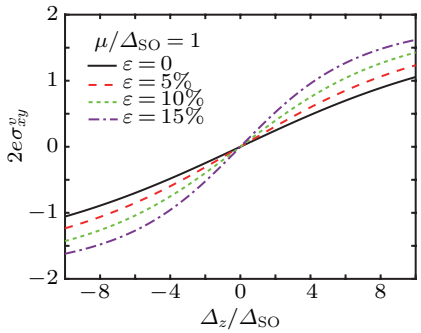


Fig. 5. (color online) VHC as a function of the electric field for different strain modulus at $\mu/\Delta_{SO} = 1$.

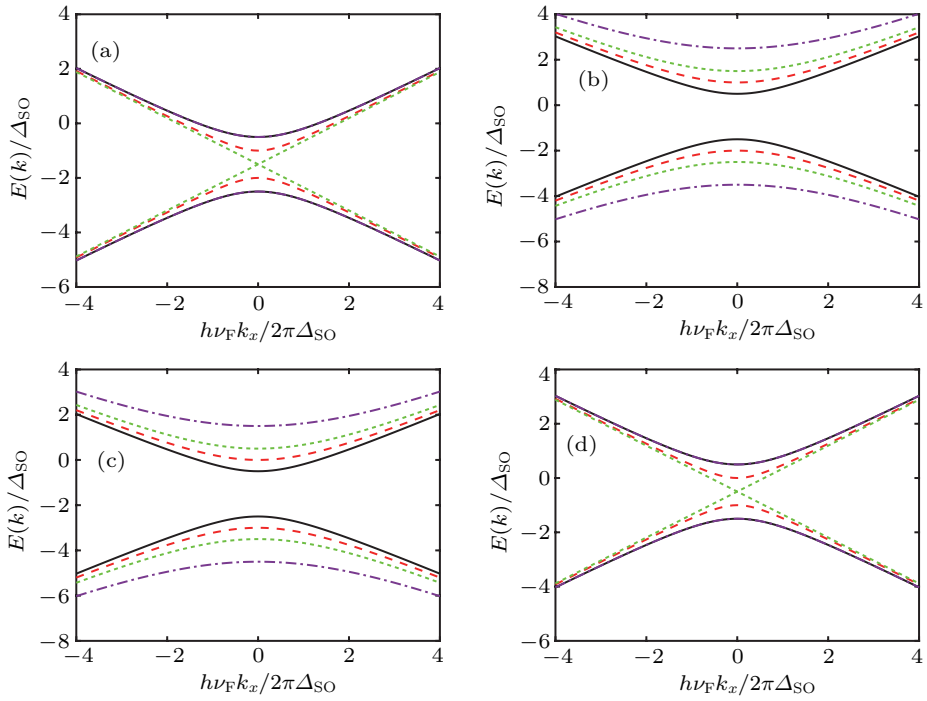


Fig. 6. (color online) The energy spectrum of ferromagnetic silicene with $M = \Delta_{SO}/2$ and $\varepsilon = 0.07 = 7\%$ for different electric field strengths ($E_z = \Delta_z/d$): $\Delta_z/\Delta_{SO} = 0$ (black solid lines), $\Delta_z/\Delta_{SO} = 0.5$ (red dashed lines), $\Delta_z/\Delta_{SO} = 1$ (green dotted lines), and $\Delta_z/\Delta_{SO} = 2$ (violet dotdashed lines). (a) Valley K, $s_z = +$; (b) valley K, $s_z = -$; (c) valley K', $s_z = +$; (d) valley K', $s_z = -$.

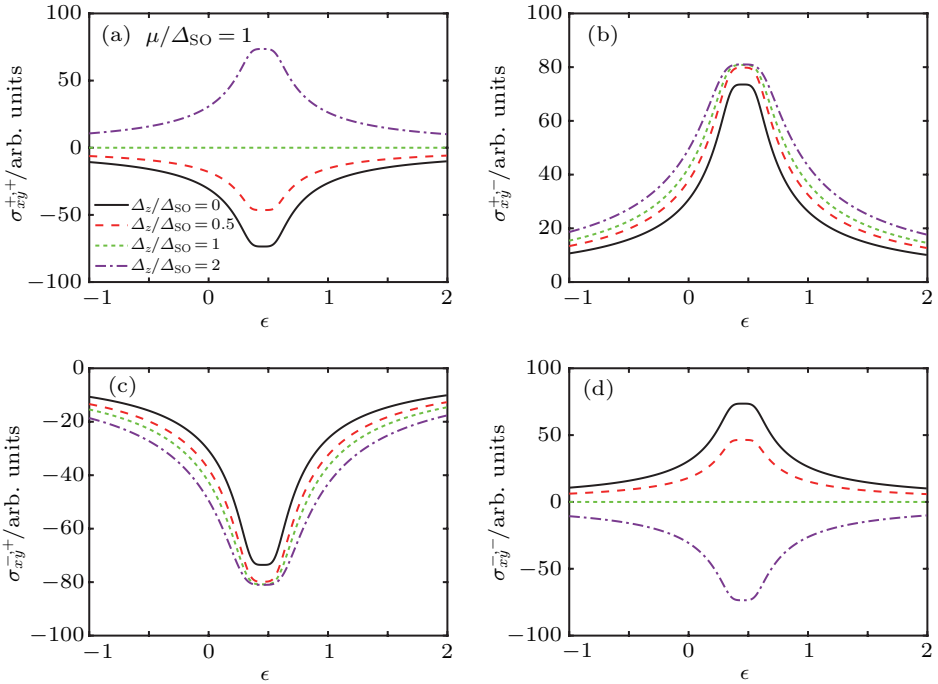


Fig. 7. (color online) The DC transverse Hall conductivity ((a) $\sigma_{xy}^{+,+}$, (b) $\sigma_{xy}^{+,-}$, (c) $\sigma_{xy}^{-,+}$, (d) $\sigma_{xy}^{-,-}$) as a function of strain for different applied electric fields and all spin and valley configurations with $\mu/\Delta_{SO} = 1$.

A plot of the band structure evolution around the K and K' points for various Δ_z/Δ_{SO} is shown in Fig. 6. Due to the symmetry between valleys, the spin labels switch at the K' point. For $\Delta_z/\Delta_{SO} = 0$, in the presence of the strain $\varepsilon = 0.07 = 7\%$, the spin degeneration of all energy bands is broken and separated by an insulating gap of Δ_{SO} (black solid lines). By increasing the electric field such that $\Delta_z < \Delta_{SO}$, the system behavior is similar to a topological insulator (TI) and the system has two different behaviors for spin up and down at K and K' valleys. For spin up (down) at K (K'), the gap decreases; and for spin down (up) at K (K'), it increases with Δ_z/Δ_{SO}. When Δ_z reaches to Δ_{SO}, i.e., $\Delta_z = \Delta_{SO}$, the band gap closes; by

increasing Δ_z further, a transition to the band insulator phase occurs; then the band gap reopens, which is in agreement with the mentioned work by Nicol and Tabert. It is necessary to point out that this occurs only for valley K (K') with spin up (down) and this transition has a main role in the study of transport properties. For valley K (K') with spin down (up), the band gap slightly increases with the electric field.

Figure 7 shows the behavior of the DC Hall conductivity with strain for various electric fields. For all cases, the conductivity is symmetric about a critical strain around $\varepsilon = 0.45 = 45\%$. For valley K (K') with spin up (down), the conductivity increases (decreases) with the electric field and is zero at $\Delta_z = \Delta_{SO}$ due to the phase transition. Before this critical strain, the conductivity decreases (increases) for $\Delta_z < \Delta_{SO}$ and then increases (decreases) with the strain. On the other hand, for valley K (K') with spin down (up), the conductivity increases (decreases) with the electric field slightly. Furthermore, it increases (decreases) with the strain before (after) the critical strain for valley K with spin down, while its behavior is inverse for valley K' with spin up. Contrary to the case $\Delta_z \leq \Delta_{SO}$, the conductivity has a positive value for $\Delta_z > \Delta_{SO}$ due to the mentioned phase transition for valley K (K') with spin up (down). According to the previous explanations, SHC is zero for $2 < \varepsilon < -1$ (the negative value for ε means compressive) and is increasing with the electric field as in the topological insulator state has a $-\hbar/2e$ value by considering the arbitrary units for the DC Hall conductivity at $\Delta_z = \Delta_{SO}$, as shown in Fig. 8. Another point is related to the SHC at $\Delta_z = 0$, which has the minimum value $(-1.85\hbar/2e)$ in agreement with Refs. [22] and [56]. For $\Delta_z > \Delta_{SO}$ in the band insulator phase, SHC has a symmetric behavior with respect to the critical strain and becomes zero near this critical point. Also the VHC has the same behavior around the critical strain with the electric field. It is zero at $\Delta_z = 0$ and $1/2e$ at $\Delta_z = \Delta_{SO}$, as presented in Fig. 9.

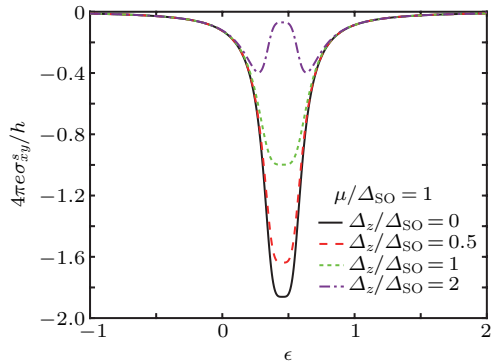


Fig. 8. (color online) SHC as a function of the strain for different applied electric fields with $\mu/\Delta_{SO} = 1$.

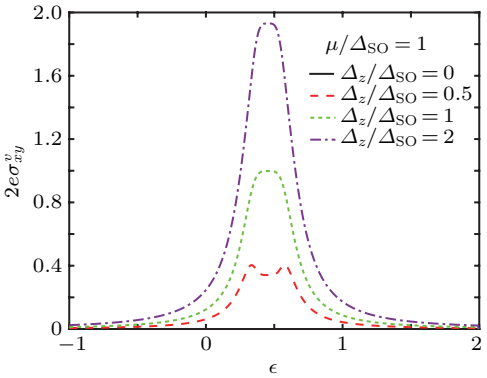


Fig. 9. (color online) VHC as a function of the strain for different applied electric fields with $\mu/\Delta_{SO} = 1$.

5. Conclusion

Kubo formalism has been used to study the low energy electronic structure and SHC-VHC of a doped ferromagnetic silicene under strain in the presence of an electric field. It is found that SHC symmetrically decreases (increases) with respect to the direction of the applied electric field while VHC increases independently. A phase transition from topological insulator to band insulator occurs with the electric field in the presence of a fixed strain. The same behavior is observed for SHC with strain at a critical strain about $\varepsilon = 45\% = 0.45$, while VHC symmetrically increases (decreases) with the strain. Eventually, the phase transition for SHC and VHC is confirmed here in comparison with the previous works.

References

[1] Novoselov K S, Geim A K, Morozov S V, Jiang D, Zhang Y, Dubonos S V, Grigorieva I V and Firsov A A 2004 *Science* **306** 666
[2] Mak K F, Lee C, Hone J, Shan J and Heinz T F 2010 *Phys. Rev. Lett.* **105** 136805
[3] Castro Neto A H, Guinea F, Peres N M R, Novoselov K S and Geim A K 2009 *Rev. Mod. Phys.* **81** 109
[4] Peres N M R 2010 *Rev. Mod. Phys.* **82** 2673
[5] Pacile D, Meyer J C, Girit C O and Zettl A 2008 *Appl. Phys. Lett.* **92** 133107
[6] Novoselov K S, Jiang D, Schedin F, Booth T J, Khotkevich V V, Morozov S V and Geim A K 2005 *Proc. Natl. Acad. Sci. USA* **102** 10451
[7] Yarmohammadi M 2016 *J. Electron. Mater.* **45** 4958
[8] Semenoff G W 1984 *Phys. Rev. Lett.* **53** 2449
[9] Katsnelson M I, Novoselov K S and Geim A K 2006 *Nat. Phys.* **2** 620
[10] Yarmohammadi M and Zareyan M 2016 *Chin. Phys. B* **25** 068105
[11] Lin Y, Jenkins K A, Valdes-Garcia A, Small J P, Farmer D B and Avouris P 2009 *Nano Lett.* **9** 422
[12] Kedzierski J, Hsu P, Healey P, Wyatt P W, Keast C L, Sprinkle M, Berger C and Heer WA de 2008 *IEEE Trans. Electron. Devices* **55** 2078
[13] Lalmi B, Oughaddou H, Enriquez H, Kara A, Vizzini S, Ealet B and Aufray B 2010 *Appl. Phys. Lett.* **97** 223109
[14] Padova P E, Quaresima C, Ottaviani C, Sheverdyaeva P M, Moras P, Carbone C, Topwal D, Olivieri B, Kara A, Oughaddou H, Aufray B and Lay G L 2010 *Appl. Phys. Lett.* **96** 261905
[15] Aufray B, Vizzini A, Oughaddou H, Lndri C, Ealet B and Lay G L 2010 *Appl. Phys. Lett.* **96** 183102
[16] Vogt P, Padova P De, Quaresima C, Frantzeskakis J A E, Asensio M C, Resta A, Ealet B and Lay G L 2012 *Phys. Rev. Lett.* **108** 155501
[17] Drummond N D, Z'olyomi V and Fal'ko V I 2012 *Phys. Rev. B* **85** 075423

[18] Ni Z, Liu Q, Tang K, Zheng J, Zhou J, Qin R, Gao Z, Yu D and Lu J 2012 *Nano Lett.* **12** 113
[19] Liu C C, Feng W and Yao Y 2011 *Phys. Rev. Lett.* **107** 076802
[20] Drummond N D, Z'olyomi V and Fal'ko VI 2012 *Phys. Rev. B* **85** 075423
[21] Ezawa M 2012 *New J. Phys.* **14** 033003
[22] Ezawa M 2012 *Phys. Rev. Lett.* **109** 055502
[23] An X T, Zhang Y Y, Liu J J and Li S S 2012 *New J. Phys.* **14** 083039
[24] Tahir M and Schwingenschlogl U 2013 *Sci. Rep.* **3** 1075
[25] Ezawa M 2013 *Phys. Rev. Lett.* **110** 026603
[26] Tsai W F, Huang C Y, Chang T R, Lin H, Jeng H T and Bansil A 2013 *Nat. Commun.* **4** 1500
[27] Tabert C J and Nicol E J 2013 *Phys. Rev. Lett.* **110** 197402
[28] Pan H, Li Z, Liu C C, Zhu G, Qiao Z and Yao Y 2014 *Phys. Rev. Lett.* **112** 106802
[29] Yarmohammadi M 2016 *AIP Advances* **6** 085008
[30] Gui G, Li J and Zhong J 2008 *Phys. Rev. B* **78** 075435
[31] Pereira V M, Castro Neto A H and Peres N M R 2009 *Phys. Rev. B* **80** 045401
[32] Choi S M, Jhi S H and Son Y W 2010 *Phys. Rev. B* **81** 081407R
[33] Farjam M and Rafii-Tabar H 2009 *Phys. Rev. B* **80** 167401
[34] Liu G, Wu M S, Ouyang C Y and Xu B 2012 *Europhys. Lett.* **99** 17010
[35] Wang Y and Ding Y 2013 *Solid State Commun.* **155** 6
[36] Kaloni T P, Cheng Y C and Schwingenschlogl U 2013 *J. Appl. Phys.* **113** 104305
[37] Mohan B, Kumar A and Ahluwalia P K 2014 *Physica E* **61** 40
[38] Zhao H 2012 *Phys. Lett. A* **376** 3546
[39] Pesin D and MacDonald A H 2012 *Nat. Mater.* **11** 409
[40] Rycerz A, Tworzydlo J and Beenakker J C W 2007 *Nat. Phys.* **3** 172
[41] Grujic M M, Tadic M Z and Peeters F M 2014 *Phys. Rev. Lett.* **113** 046601
[42] Moldovan D, Ramezani Masir M, Covaci L and Peeters F M 2012 *Phys. Rev. B* **86** 115431
[43] Song Y, Zhai F and Guo Y 2013 *Appl. Phys. Lett.* **103** 183111
[44] Zhang L and Wang J 2014 *Chin. Phys. B* **23** 087202
[45] Tian H Y and Wang J 2012 *Chin. Phys. B* **21** 017203
[46] Sasaki K I and Saito R 2008 *Prog. Theor. Phys. Supp.* **176** 253
[47] Pereira V M and Castro Neto A H 2009 *Phys. Rev. Lett.* **103** 046801
[48] Fujita T, Jalil M B A and Tan S G 2010 *Appl. Phys. Lett.* **97** 043508
[49] Chaves A, Covaci L, Rakhimov K Y, Farias G A and Peeters F M 2010 *Phys. Rev. B* **82** 205430
[50] Niu Z P 2012 *J. Appl. Phys.* **111** 103712
[51] Liu C C, Feng W and Yao Y 2011 *Phys. Rev. Lett.* **107** 076802
[52] Tahir M, Manchon A, Sabeeh K and Schwingenschlogl U 2013 *Appl. Phys. Lett.* **102** 162412
[53] Stille L, Tabert C J and Nicol E J 2012 *Phys. Rev. B* **86** 195405
[54] Tabert C J and Nicol E J 2013 *Phys. Rev. B* **87** 235426
[55] An X T, Zhang Y Y, Liu J J and Li S S 2013 *Appl. Phys. Lett.* **102** 043113
[56] Dyrda A and Barnas J 2012 *Phys. Status Solidi* **6** 340
[57] Yokoyama T 2013 *Phys. Rev. B* **87** 241409
[58] Haugen H, Huertas-Hernando D and Brataas A 2008 *Phys. Rev. B* **77** 115406
[59] Qiao Z, Yang S A, Feng W, Tse W K, Ding J, Yao Y, Wang J and Niu Q 2010 *Phys. Rev. B* **82** 161414
[60] Pereira V M, Castro Neto A H and Peres N M R 2009 *Phys. Rev. B* **80** 045401
[61] Wang B, Wu J, Gu X, Yin H, Wei Y, Yang R and Dresselhaus M 2014 *Appl. Phys. Lett.* **104** 081902
[62] Pellegrino F M D, Angilella G G N and Pucci R 2012 *Phys. Rev. B* **85** 195409
[63] Sattari F 2016 *J. Magn. Magn. Mater.* **414** 19
[64] Vargiamidis V, Vasilopoulos P and Hai G Q 2014 *J. Phys. Condens. Matter.* **26** 345303
[65] Kane C L and Mele E J 2005 *Phys. Rev. Lett.* **95** 226801
[66] Sinitsyn N A, Hill J E, Min H, Sinova J and MacDonald A H 2006 *Phys. Rev. Lett.* **97** 106804
[67] Li Z and Carbotte J P 2012 *Phys. Rev. B* **86** 205425
[68] Rakshit B and Mahadevan P 2010 *Phys. Rev. B* **82** 153407
[69] Qin R, Wang C, Zhu W and Zhang Y 2012 *AIP Advances* **2** 022159
[70] Tabert C J and Nicol E J 2013 *Phys. Rev. B* **88** 085434
[71] Tahir M, Manchon A, Sabeeh K and Schwingenschlogl U 2013 *Appl. Phys. Lett.* **102** 162412